Search for Kaluza-Klein excitations of the gluon in models with extra dimensions

L. March, E. Ros, B. Salvachúa

IFIC, University of Valencia/CSIC, Spain

Abstract

The decay of Kaluza-Klein excitations of the gluon is analyzed in the context of some extra-dimension models. The mass of these excitations is assumed to be in the region of a few TeV and decays involving b and t quarks are investigated.

ATL-PHYS-PUB-2006-002
03 January 2006

1 Introduction

Kaluza-Klein (KK) excitations of gauge bosons are predicted in the context of some models with TeV^{-1} size extra-dimensions. Examples of such models are variants of the so called 'ADD model' [1], with fermions confined to a D-brane, but with the difference that all gauge bosons may propagate in the bulk. The phenomenology of such models is discussed for example in [2]. The potential of ATLAS to observe KK excitations of the weak gauge bosons (Z and W) has already been discussed in [3] and [4]. KK gluon excitations are also expected as discussed in [5]. The KK excitations of Z and W are detected by reconstructing their leptonic decays. The detection of KK excitations of the gluon is much more challenging since only hadronic decays are expected. The sensitivity of LHC for such gluon excitations (g^* in the following) has already been discussed in [6]. In these searches, the presence of gluon excitations is detected by analyzing deviations in the dijet cross-section. An alternative is proposed in the present analysis, where the presence of g^* is detected by analyzing its decays into heavy quarks.

2 Cross-sections and Branching ratios

According to [5], the couplings of g^* to quarks are equal to the Standard Model couplings of the gluon to quarks, except for the presence of an additional $\sqrt{2}$ factor. Therefore, the gluon excitations appear as wide resonances decaying into pairs of quarks. The width is expected to be

$$\Gamma(g^*) = 2\alpha_{\mathrm{s}}\mathrm{M},$$

where M is the mass of g^*. This width is of the order of 200 GeV for a mass M = 1 TeV. The production cross-section of these g^* resonances is complicated, since one has to consider several Feynman diagrams including s, t and u channels, as discussed in [5]. This complexity requires the use of dedicated MC programs, as discussed in [6]. Since in the present analysis only decays to heavy quarks are considered, the production mechanism includes a single diagram in the s-channel ($q_i\bar{q_i} \rightarrow g^* \rightarrow Q_i\bar{Q}_i$, where q_i is a light quark and Q_i a heavy quark). The cross-section can be computed numerically and the events can be generated in a simple way by modifying the couplings of a heavy gauge boson in the Pythia MC program [7].

The cross-sections obtained in this way are reported in Table 1. All cross-sections are computed at leading order (LO). In these computations the energy scale is equal to the mass of the resonance ($\mathrm{Q}^2 = \mathrm{M}^2$) and CTEQ5L pdf's are selected.

Table 1. Cross-sections at LHC for g^* production.

M (GeV)	$\sigma(g^*)$ (pb)
1000	1109
1500	192
2000	47
3000	4.9

As a consequence of gauge symmetry, all couplings of g^* to quarks are equal. If the mass of g^* is large enough, all quark masses can be neglected and the branching ratios (BR) of g^* to heavy quarks are:

$$BR(g^* \rightarrow b\bar{b}) = BR(g^* \rightarrow t\bar{t}) = 1/6 = 16.7\%.$$

3 Event simulation

The analysis of the present note follows closely the analysis presented in reference [8], where more details about selection cuts and backgrounds can be found.

Most of the events used in the present analysis have been generated using the MC program PYTHIA coupled to ATLFAST [9] to simulate the detector response. The MC program ALPGEN [10] has been used as well to generate background events containing $W + jets$. In the ALPGEN MC program, the exact matrix elements are used for multijet production. The following sets of events were used in this analysis:

- **Signal:** $g^* \to b\bar{b}$ and $t\bar{t}$ with g^* masses in the range between 1 and 3 TeV.
- **Background:** Standard Model final states containing $b\bar{b}$, $t\bar{t}$, $2jets$ and $W + jets$. Since only events with very high p_{T} jets and large center of mass energy are relevant in this analysis, it was imposed at the generation level that

$$\sqrt{\hat{s}} > 0.5(1.0)\,\mathrm{TeV} \text{ and } \hat{p}_{\mathrm{T}} > 0.1(0.25)\,\mathrm{TeV},$$

  where $\sqrt{\hat{s}}$ and $\hat{p}_{\mathrm{T}}$ are the center-of-mass energy and transverse momentum of the hard process. The low cuts were used in the background estimation for M = 1 and 1.5 TeV and the high cuts for M = 2 and 3 TeV.

Table 2 summarizes the number of signal events generated and Table 3 the cross-sections and the number of events for background sources. In PYTHIA, dijet events containing light quarks (jj) and heavy quarks ($b\bar{b}$ and $t\bar{t}$) are generated using different processes. Heavy quarks may appear in the light quark sample as a result of gluon splitting but these events are excluded in the present analysis.

Table 2. Number of generated events for $g^* \to b\bar{b}$ and $g^* \to t\bar{t}$.

M (TeV)	$g^* \to b\bar{b}$	$g^* \to t\bar{t}$
1.0	10 000	100 000
1.5	10 000	30 000
2.0	10 000	10 000
3.0	—	10 000

In case KK excitations of g exist, KK excitations of Z and γ are also expected and their decays to heavy quarks will reinforce the g^* signal. This additional signal is however small and is not considered in the present analysis.

Table 3. Cross-sections and generated events containing $b\bar{b}, jj, t\bar{t}$ and $W + jets$.

	σ (pb)		Number of Events	
	Low cuts	High cuts	Low cuts	High cuts
$b\bar{b}$	391	7.7	100 000	100 000
jj	303 000	5 700	100 000	100 000
$t\bar{t}$	164	6.35	100 000	100 000
$W + jets$ (ALPGEN)	161	30	112 700	113 300
$W + jets$ (PYTHIA)	42.4	1.77	100 000	100 000

4 Event analysis

The analysis of the events follows closely a similar analysis performed in [8] and a summary is given below. For the analysis of the decay $g^* \rightarrow b\bar{b}$, the following cuts are applied:

- $|\eta| < 2.5$ and 2 b-jets with p_{T} cuts shown in Table 4.

Table 4. Cuts applied to b-jets in the channel $g^* \rightarrow b\bar{b}$.

p_{T} (GeV)	M = 1 TeV	M = 1.5 TeV	M = 2 TeV
b-jet 1	350	525	700
b-jet 2	150	225	300

The b-tagging of very high p_{T} jets is discussed in the Appendix. Two background sources have been analyzed: $b\bar{b}$ production (irreducible background) and 2-jet production (reducible background).

For the analysis of the decay $g^* \rightarrow t\bar{t}$, the following cuts are applied, assuming that one of the t-quarks decays leptonically:

- A lepton (electron or muon) with $p_{\mathrm{T}} > 25\,\mathrm{GeV}$ and $|\eta| < 2.5$, in addition to $(E_{\mathrm{T}})_{miss} > 25\,\mathrm{GeV}$.
- 2 b-jets with $p_{\mathrm{T}} > 25\,\mathrm{GeV}$ and $|\eta| < 2.5$, the first jet such that $\Delta\mathrm{R}(b\text{-lepton}) < 2$ and the second such that $\Delta\mathrm{R}(b\text{-lepton}) > 2$. The distance $\Delta\mathrm{R}$ is defined in the usual way as

$$\Delta\mathrm{R} = \sqrt{(\Delta\phi)^2 + (\Delta\eta)^2},$$

where ϕ is the azimuth and η the rapidity.

- The first t-quark is reconstructed using the first b-jet, the lepton and the missing energy, assuming that the missing neutrino is parallel to the lepton. The second t-quark is reconstructed using the second b-jet and all other reconstructed jets, within a distance of 2. The p_{T} of the reconstructed t-quarks should be larger than the cut values reported in Table 5 for M = 1, 1.5, 2 and 3 TeV.

Table 5. Cuts applied to t-jets in the channel $g^* \to t\bar{t}$.

p_{T} (GeV)	M = 1 TeV	M = 1.5 TeV	M = 2 TeV	M = 3 TeV
t-jet 1	350	525	700	1050
t-jet 2	150	225	300	450

The kinematical efficiencies achieved for signal events with the selection cuts described before are summarized in Table 6.

The reconstructed mass peaks are shown in Fig. 1(a) and 1(b), for the b-quark channel, and in Fig. 2(a) to 2(d), for the t-quark channel. The corresponding mean values and widths resulting from Gaussian fits are reported in Table 7.

Table 6. Kinematical efficiencies (all BR and tagging efficiencies excluded).

M (TeV)	$g^* \to b\bar{b}$	$g^* \to t\bar{t}$
1.0	35%	14%
1.5	32%	12%
2.0	31%	10%
3.0	—	3%

Table 7. Central value of the reconstructed mass (M) and width ($\pm\Delta$M) for the various decay channels analyzed. All values are in GeV.

M (TeV)	$g^* \to b\bar{b}$	$g^* \to t\bar{t}$
1.0	999 ± 161	967 ± 147
1.5	1504 ± 254	1504 ± 220
2.0	1995 ± 329	2050 ± 306
3.0	—	2990 ± 520

Since the natural width of g^* is 200 GeV for M = 1 TeV, both the natural width and experimental effects (fragmentation and detector resolution) contribute to the mass peak, and these contributions are approximately equal.

Fig. 3 and 4 display the invariant mass distributions, including the signal on top of the expected background. By applying mass cuts of $\pm$200, $\pm$300, $\pm$400

and $\pm 600\,\mathrm{GeV}$ around the expected mass values of M = 1, 1.5, 2 and 3 TeV, respectively, it is possible to obtain the number of signal and background events which are reported in Tables 8 and 9, for an integrated luminosity of $\mathcal{L} = 3 \cdot 10^5\,\mathrm{pb}^{-1}$, corresponding to 3 years of running of high luminosity. The significance of the expected signal is indicated as well. In the $g^* \to t\bar{t}$ channel, the reducible background is composed of $W + jets$ events. This background can be calculated using both PYTHIA and ALPGEN. The values obtained with ALPGEN are considerably larger and have been used, in a conservative approach, to calculate the various significances.

Table 8. Signal and background for $g^* \to b\bar{b}$ assuming $\mathcal{L} = 3 \cdot 10^5\,\mathrm{pb}^{-1}$.

M (TeV)	Signal	Irreducible bkg	Reducible bkg	Significance
1.0	192412	48562	47099	622
1.5	30720	6018	41394	141
2.0	7168	1174	26970	43

Table 9. Signal and background for $g^* \to t\bar{t}$ assuming $\mathcal{L} = 3 \cdot 10^5\,\mathrm{pb}^{-1}$.

M (TeV)	Signal	Irreducible bkg	Reducible bkg (ALPGEN)	Reducible bkg (PYTHIA)	Significance (ALPGEN)
1.0	505413	44612	493	48	2379
1.5	27838	1926	52	1.77	626
2.0	2318	174	12	1.01	170
3.0	80.3	8.9	10.5	0.95	18.2

Fig. 5 and 6 show the significance as a function of the g^* mass. Assuming an exponential dependence of the significance on the mass, it is possible to conclude that a significance of 5 may be achieved below M = 2.7 TeV and M = 3.3 TeV, for $g^* \to b\bar{b}$ and $t\bar{t}$, respectively. On the other hand, it is not possible in general to obtain mass peaks well separated from the background. Therefore, it is unlikely that an excess of events in the channel $g^* \to b\bar{b}$ could be used as an evidence for the presence of the g^* resonance, since there are large uncertainties in the calculation of the backgrounds. For M = 1 TeV, the peak displacement (see Fig. 3(a)) could be used as an evidence for new physics if the b-jet energy scale can be accurately computed.

In the $g^* \to t\bar{t}$ case, on the contrary, the background is mainly irreducible and not so large, so the g^* resonance can be detected in this decay channel if the $t\bar{t}$ cross-section can be computed in a reliable way.

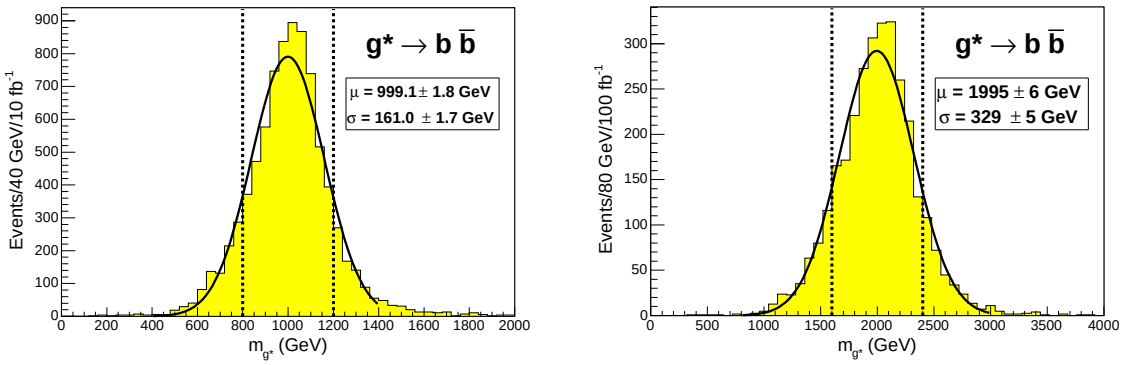

(a) (b)

Fig. 1. Reconstructed mass peaks for $g^* \to b\bar{b}$ and mass values of M = 1 and 2 TeV. The curves on top of the data are Gaussian fits.

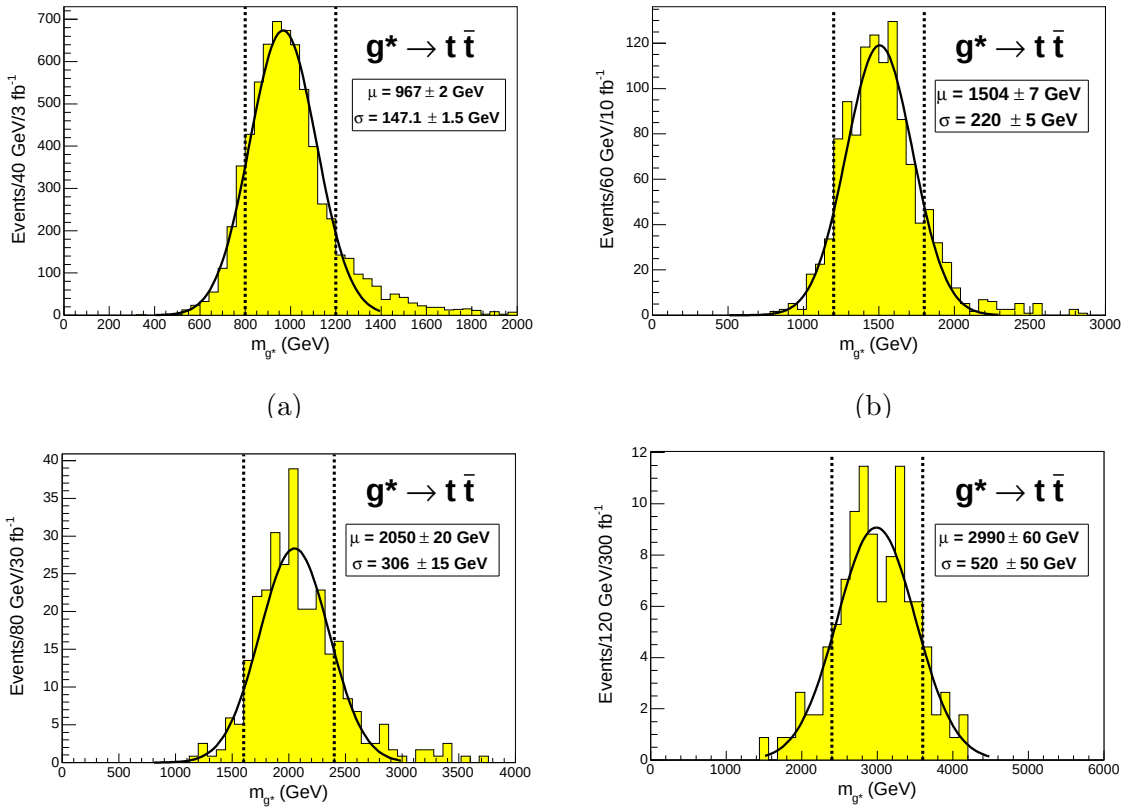

(a) (b)

(c) (d)

Fig. 2. Reconstructed mass peaks for $g^* \to t\bar{t}$ and mass values of M = 1, 1.5, 2 and 3 TeV. The curves on top of the data are Gaussian fits.

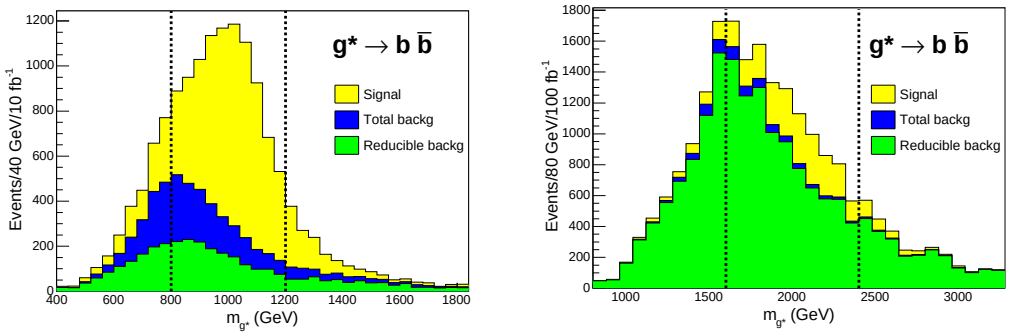

(a) (b)

Fig. 3. Reconstructed mass peaks for $g^* \to b\bar{b}$ including both signal and background contributions for mass values of M = 1 and 2 TeV. The mass window used to calculate the significance is indicated in the figures. Luminosities of $\mathcal{L} = 10^4\,\mathrm{pb}^{-1}$ and $\mathcal{L} = 10^5\,\mathrm{pb}^{-1}$ are assumed for M = 1 and 2 TeV, respectively.

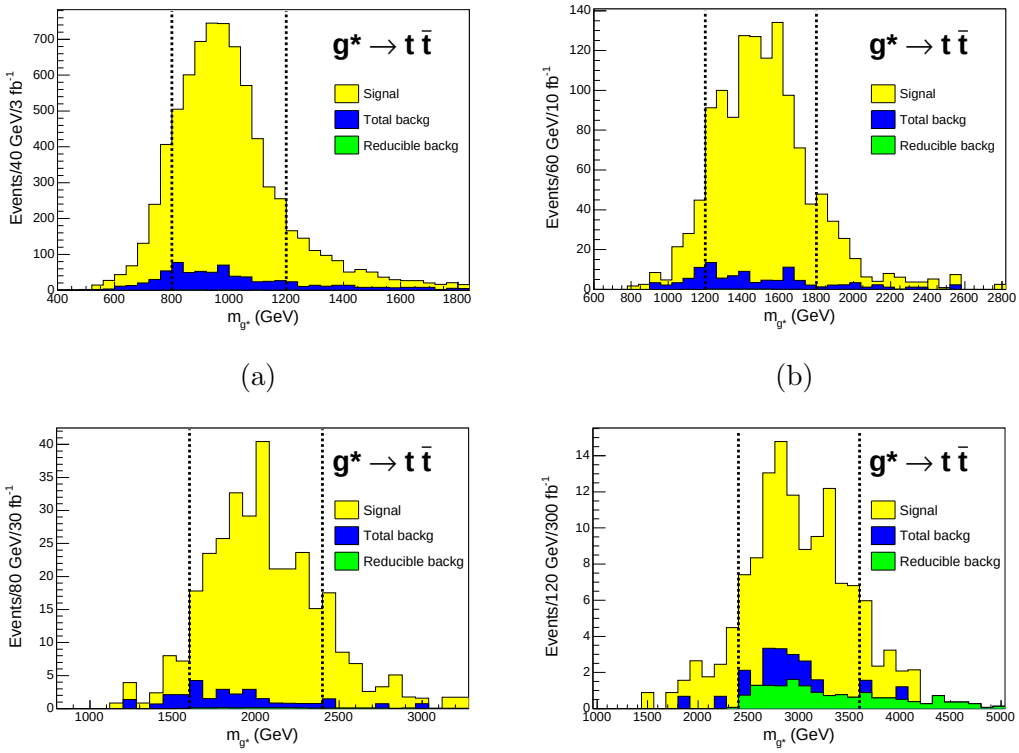

(a) (b)

(c) (d)

Fig. 4. Reconstructed mass peaks for $g^* \to t\bar{t}$ including both signal and background contributions for mass values of M = 1, 1.5, 2 and 3 TeV. The mass window used to calculate the significance is indicated in the figures. Luminosities of $\mathcal{L} = 3{\cdot}10^3\,\mathrm{pb}^{-1}$, $\mathcal{L} = 10^4\,\mathrm{pb}^{-1}$, $\mathcal{L} = 3 \cdot 10^4\,\mathrm{pb}^{-1}$ and $\mathcal{L} = 3 \cdot 10^5\,\mathrm{pb}^{-1}$ are assumed for M = 1, 1.5, 2 and 3 TeV, respectively.

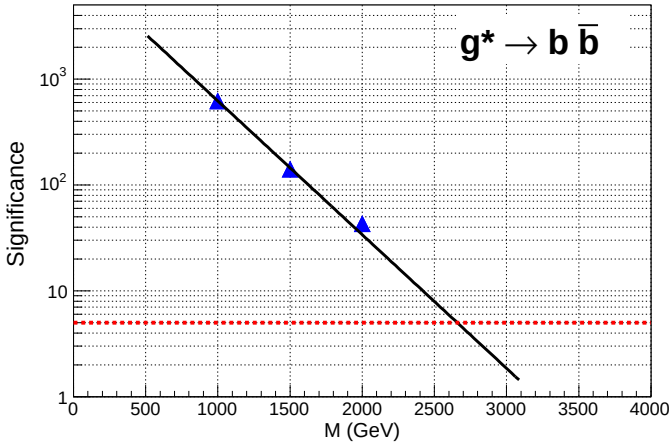

Fig. 5. Significance as a function of mass for $g^* \rightarrow b\bar{b}$ and a luminosity of $\mathcal{L} = 3 \cdot 10^5\,\mathrm{pb}^{-1}$. An exponential curve is fitted to the calculated values.

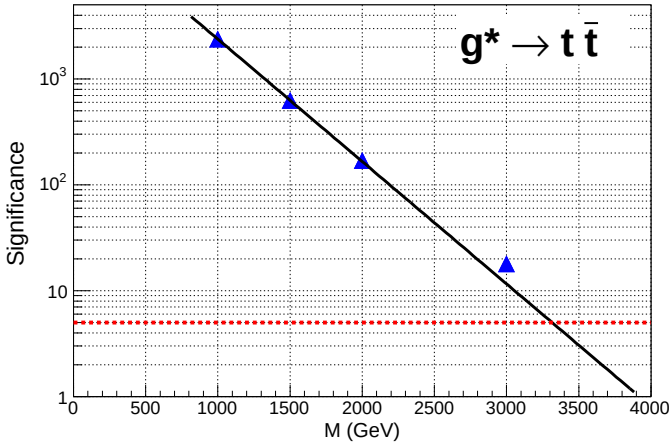

Fig. 6. Significance as a function of mass for $g^* \rightarrow t\bar{t}$ and a luminosity of $\mathcal{L} = 3 \cdot 10^5\,\mathrm{pb}^{-1}$. An exponential curve is fitted to the calculated values.

5 Summary and conclusions

The decays $g^* \to b\bar{b}$ and $g^* \to t\bar{t}$ have been investigated using the simulation program ATLFAST for g^* masses in the range between 1 and 3 TeV. The analysis of expected signals and backgrounds shows that the decays into b-quarks are difficult to detect, but the decays into t-quarks, on the contrary, might yield a significant signal for the g^* mass below 3.3 TeV. This signal could be used to confirm the presence of g^*, in case that an excess of events is observed in the dijet cross-section as proposed in [5].

Acknowledgements

We would like to thank Javier Sánchez, George Azuelos and Samir Ferrag for help and comments.

A Appendix: High p_{T} b-tagging

In all the decays analyzed in this note, the tagging of very high p_{T} b-jets is required. The average p_{T} of these jets is reported in Table A.1

Table A.1. Average p_{T} of final state b-jets for the various channels.

M (TeV)	$< p_{\mathrm{T}} >$ (GeV) $g^* \to b\bar{b}$	$< p_{\mathrm{T}} >$ (GeV) $g^* \to t\bar{t}$
1.0	400	200
1.5	600	300
2.0	800	400
3.0	—	600

The tagging of very high p_{T} jets has already been discussed in [8]. Table A.2 shows all efficiencies and rejections used in the present analysis.

Table A.2. Efficiencies and rejections applied in the b-tagging analysis.

M (TeV)	decay	ϵ_b	R_c	R_u	decay	ϵ_b	R_c	R_u
1.0	$b\bar{b}$	0.1	100	400	$t\bar{t}$	0.5	10	100
1.5	$b\bar{b}$	0.1	50	90	$t\bar{t}$	0.3	24	200
2.0	$b\bar{b}$	0.1	30	50	$t\bar{t}$	0.2	30	130
3.0	$b\bar{b}$	—	—	—	$t\bar{t}$	0.2	13	30

References

[1] N. Arkani-Hamed, S. Dimopoulos and G. R. Dvali,
Phys. Rev. **D59** (1999) 086004.

[2] G. Rizzo,
Phys. Rev. **D61** (2000) 055005.

[3] G. Azuelos and G. Polesello,
Eur. Phys. J. **C39S2** (2005) 1-11.

[4] G. Polesello and M. Prata,
Eur. Phys. J. **C32S2** (2003) 55-67.

[5] D. A. Dicus, C. D. McMullen and S. Nandi,
Phys. Rev. **D65** (2002) 076007.

[6] C. Balazs, M. Escalier, S. Ferrag, B. Laforge and G. Polesello,
The sensitivity of the LHC for TeV scale dimensions in dijet production, prepared for 3rd Les Houches Workshop, Physics at TeV Colliders,
Les Houches, France, 26 May - 6 June 2003.

[7] T. Sjostrand et al.,
Comput. Phys. Commun. **135** (2001) 238-259.

[8] S. González de la Hoz, L. March and E. Ros,
Search for hadronic decays of Z_{H} and W_{H} in the Little Higgs model,
ATLAS Communication, ATL-COM-PHYS-2005-001 (submitted as physics note).

[9] E. Richter-Was, D. Froideveaux and L. Poggioli,
ATLFAST 2.0 a fast simulation package for ATLAS,
ATLAS Internal Note, ATL-PHYS-98-131.

[10] M. L. Mangano et al.,
ALPGEN, a generator for hard multiparton processes in hadronic collisions,
JHEP **07** (2003) 001.